Optimization for Power Distribution and Maintenance Schedules of Paralleled Transmission Channels in AC/DC Power System

Jie Liu, Shunjiang Lin, *Senior Member*, *IEEE*, Weikun Liang, Yanghua Liu, and Mingbo Liu, *Member*, *IEEE*

***Abstract*——As transmission power among interconnected regional grids is increasing rapidly, formulating the power distribution and maintenance schedules of multiple paralleled transmission channels are critical to ensure the secure and economic operation in an AC/DC power system. A coordinated optimization for power distribution and maintenance schedules (COPD-MS) of multiple paralleled transmission channels is proposed, and the active power losses of the resistances of earth line in the high-voltage direct current (HVDC) transmission lines are taken into account when one pole is under maintenance while the other pole is operating under monopolar ground circuit. To solve the proposed COPD-MS model efficiently, the generalized Benders decomposition (GBD) algorithm is used to decompose the proposed COPD-MS model into master problem of maintenance scheduling and sub-problems of power distribution scheduling, and the optimal solution of the original model is obtained by the alternative iteration between them. Moreover, a recursive acceleration (RA) algorithm is proposed to solve the master problem, which can directly obtain its solution in the new iteration by using the solution in the last iteration and the newly added Benders cut. Convex relaxation techniques are applied to the nonlinear constraints in the sub-problem to ensure the reliable convergence. Additionally, since there is no coupling among the power distributions during each time interval in the sub-problem, parallel computing technology is used to improve the computational efficiency. Finally, case studies on the modified IEEE 39-bus system and an actual 1524-bus large-scale AC/DC hybrid power system demonstrate the effectiveness of the proposed COPD-MS model.**

***Index Terms*—AC/DC power system, power distribution schedule, transmission maintenance schedule, generalized Benders decomposition (GBD), recursive acceleration (RA).**

NOMENCLATURE

A. Sets and Indices

Ω_R	Set of poles of DC transmission line connected to rectifier station
Ω_{I_1}, Ω_{I_2}	Sets of poles of DC transmission line connected to inverter station
Ω_{ar}, Ω_{dr}	Sets of AC and DC transmission lines in transmission section r
Ω_k	Set of branches included in the k^{th} independent circuit
i, j	Indices of buses
k, N_{ac}	Index and number of AC transmission lines
l, N_{dc}	Index and number of DC transmission lines
m, Ω_m	Index and set of transmission lines under maintenance
min, max	Indices of the minimum and maximum values
N	Number of buses
N_v	Number of AC buses connected to voltage source converter based multi-terminal high-voltage direct current (VSC-MTDC) converter stations
t, T	Index and number of time periods
0	Index of initial value

B. Parameters

η%	Allowable deviation of power exchange
ε	Convergence accuracy of generalized Benders decomposition (GBD) algorithm
μ_i	DC voltage utilization ratio
ΔT	Length of each time interval
$c_{g,t}$	Electricity price of power grid at time t
$c_{m,t}$	Maintenance cost of transmission line m at time t
g_{ak}, b_{ak}	Conductance and admittance of AC transmission line k
$g'_{ak,t}$, $b'_{ak,t}$	Actual conductance and admittance of AC transmission line k at time t
G_{ij}, B_{ij}	Mutual conductance and susceptance between buses i and j

Manuscript received: December 17, 2023; revised: February 20, 2024; accepted: April 16, 2024. Date of CrossCheck: April 16, 2024. Date of online publication: May 3, 2024.

This work was supported by the National Natural Science Foundation of China (No. 51977080) and the Natural Science Foundation of Guangdong Province (No. 2022A1515010332).

This article is distributed under the terms of the Creative Commons Attribution 4.0 International License (http://creativecommons.org/licenses/by/4.0/).

J. Liu, S. Lin (corresponding author), W. Liang, and M. Liu are with the School of Electric Power Engineering, South China University of Technology, Guangzhou, China (e-mail: linshj@scut. edu. cn; 1653080768@qq. com; 3012273545@qq.com; epmbliu@scut.edu.cn).

Y. Liu is with the School of Electromechanical Engineering, Guangdong Polytechnic Normal University, Guangzhou, China (e-mail: 1148972539@qq.com).

DOI: 10.35833/MPCE.2023.001028

K_{di}, X_{ci} Converter transformer ratio and commutation reactance of line-commutated converter based high-voltage direct current (LCC-HVDC) converter station connected to bus i

$M_{\max}$ The maximum allowable number of maintenance lines

$P_{Gi,t}$, $Q_{Gi,t}$ Active and reactive power of generator on bus i at time t

$P_{Li,t}$, $Q_{Li,t}$ Active and reactive power of load on bus i at time t

$P_{\Sigma r,t}$ Power exchange schedule value of section r at time t

R_{dl} Resistance of DC transmission line l

R_{gl} Equivalent earth resistance of DC transmission line l

R_{vij} Resistance of VSC-MTDC transmission line ij

$T_{sm,\min}$ Allowed earliest start time for maintenance of transmission line m

$T_{sm,\max}$ Allowed latest start time for maintenance of transmission line m

T_{mR} Time required for maintenance of transmission line m

Y_i Admittance of VSC-MTDC converter station connected to bus i

y_{ij} Admittance of VSC-MTDC transmission line ij

C. Variables

$\delta_{i,t}$ Phase angle difference between voltage of bus i and input voltage of its connected VSC-MTDC converter station at time t

$\theta_{ij,t}$ Voltage phase difference between buses i and j at time t

$\psi_{i,t}$ Converter control angle of LCC-HVDC converter station i at time t

$\varphi_{i,t}$ Power factor angle of LCC-HVDC converter station i at time t

$\Delta P_{Lak,t}$ Power loss of AC transmission line k at time t

$\Delta P_{Ldl,t}$ Power loss of DC transmission line l at time t

$K_{pl,t}$ Number of operating poles for DC transmission line l at time t

$I_{vij,t}$ DC current of VSC-MTDC transmission line ij at time t

$M_{i,t}$ Modulation ratio of VSC-MTDC converter station i at time t

$P_{ak,t}$ Transmission power of AC transmission line k at time t

$P_{dl,t}$, $I_{dl,t}$ Transmission power and current of DC transmission line l at time t

$P_{di,t}$, $Q_{di,t}$ Active and reactive power absorbed by LCC-HVDC converter station i from AC system at time t

$P_{vi,t}$, $Q_{vi,t}$ Active and reactive power absorbed by VSC-MTDC converter station i from AC system at time t

$P_{Gs,t}$, $Q_{Gs,t}$ Active and reactive power of swing generator at time t

$P_{ak,t}$ Transmission power of AC transmission line k at time t

$P_{vij,t}$ Transmission power of VSC-MTDC transmission line ij at time t

$s_{m,t}$ Binary variable that shows whether transmission line m starts maintenance at time t

$U_{vi,t}$, $I_{vi,t}$ DC voltage and current of VSC-MTDC converter station i at time t

$U_{di,t}$, $I_{di,t}$ DC voltage and current of LCC-HVDC converter station i at time t

$V_{i,t}$ Voltage of bus i at time t

$x_{m,t}$ Binary variable indicates whether transmission line m is under maintenance at time t

I. Introduction

In recent years, long-distance, large-capacity, and extra-/ultra-high voltage AC/DC hybrid transmission technique has developed rapidly in the power system of China [1]-[3]. With the carbon peaking and carbon neutrality target proposed by Chinese government, it is necessary to develop large-capacity renewable energy stations in the western provinces and transmit electric energy to the load centers in the eastern provinces through AC/DC transmission channels. Till 2022, the State Grid Corporation of China has established 14 AC and 12 DC transmission channels, while the China Southern Power Grid has established 8 AC and 11 DC transmission channels. In China Southern Power Grid, more than 30 billion kWh electric energy is transmitted from the power plants in Yunnan and Guizhou provinces to the load centers in Guangdong province through the AC/DC transmission channels in a month. Transmitting such a large amount of electric energy will result in significant power losses. Moreover, in order to improve the secure operation of the power system, the transmission lines in the AC/DC transmission channels require preventive maintenance to eliminate the hidden faults [4], [5]. Therefore, the coordinated optimization for the power transmission and maintenance schedules of multiple transmission channels in an AC/DC power system is very important to the secure and economic operation and can reduce the impact of maintenance on the power transmission capacity of transmission channels.

The analysis of the secure and economic operation of AC/DC power systems generally adopts the optimal power flow (OPF) model [6]-[9]. The objective function in [6] and [7] is to minimize the generation cost expressed as a polynomial function with respect to the active power output of generators. Considering the control strategies of two different voltage source converters (VSCs), [8] proposes an OPF model to minimize the transmission power loss of the AC/DC power system. In [9], the objective function includes the generation cost and the system power loss. The above literature [6]-[9] only considers the active power outputs of generators as the decision variables. However, considering that the high-voltage direct current (HVDC) transmission lines can adjust the transmission power flexibly, in an AC/DC power system, the active power loss can also be reduced by scheduling the transmission power of transmission lines between regions ex-

cept for scheduling the power output of generators within each region. Currently, some studies have focused on scheduling the transmission power of transmission lines in the AC/DC power system [10]-[13]. Reference [10] establishes a multi-objective optimization model to obtain the transmission power of DC transmission lines and reactive power outputs of generators, which aims to minimize both the active power loss and the voltage deviation. Reference [11] proposes an integrated optimization approach to exploit the operational flexibility in high-voltage AC/DC hybrid transmission grid from the generator side and transmission side. In [12], a coordinated model is proposed to schedule the tie-line flows in an AC/DC power system. The objective is to minimize the dispatch cost considering the wind power uncertainty. Reference [13] proposes an optimal day-ahead power distribution model for paralleled transmission channels to minimize the total active power loss. However, in [10]-[13], only the day-ahead power distribution schedules of AC/DC transmission channels are considered, and the influence of preventive maintenance schedules of AC/DC transmission lines on the power distribution schedules is not taken into account.

Generally, the model for formulating maintenance schedules of transmission lines includes numerous integer variables, resulting in a mixed-integer programming model with low computational efficiency. Existing algorithms for solving the mixed-integer programming model can be classified into two categories: heuristic algorithms [14]-[18] and the decomposition algorithms including Lagrangian relaxation decomposition algorithm [19] and Benders decomposition algorithm [20]-[23]. Reference [14] presents a transmission maintenance scheduling model to maximize the maintenance willingness of the transmission owners, and a machine learning approach is presented to solve this model. The proposed models in [15]-[17] are formulated for the generation and transmission maintenance schedules. In [18], the progressive hedging algorithm is applied to solve the transmission maintenance scheduling model. Although heuristic algorithms can solve the model directly without depending on the model types, such algorithms require very long computational time, which makes it difficult to be applied to actual large-scale power systems. In [19], the co-optimization problem of short-term generation and transmission maintenance schedules is decoupled into three separate optimization sub-problems by Lagrangian relaxation, which include generation maintenance scheduling, transmission maintenance scheduling, and short-term security constrained unit commitment (SCUC) problems. In [20] and [21], the Benders decomposition algorithm is applied in the integrated generation and transmission maintenance scheduling model. Considering $N-1$ contingencies, [22] proposes a transmission maintenance scheduling model and adopts the Benders decomposition algorithm to solve it. The relaxation induced algorithm is proposed to solve the master problem to improve the computational efficiency. Reference [23] proposes a transmission maintenance scheduling model with maintenance resource constraints. Based on the Benders decomposition algorithm, an exact branch-and-cut algorithm is proposed. However, the above literature only focuses on the maintenance of AC transmission lines, without considering the actual situation of the maintenance of HVDC transmission lines. In actual operation, to complete the required power transmission schedules, only one pole of an HVDC transmission line is usually scheduled for maintenance, while the other pole is still operating under monopolar ground circuit. Additionally, the maintenance of VSC-based multi-terminal HVDC (VSC-MTDC) transmission systems is not taken into account in the existing publications. For the maintenance of VSC-MTDC transmission systems, when two HVDC transmission lines are both connected to rectifier or inverter stations, one HVDC transmission line is under maintenance, and the other line still operates.

This paper makes the following two contributions.

1) A coordinated optimization for power distribution and maintenance schedules (COPD-MS) of multiple paralleled transmission channels is proposed. The proposed COPD-MS model considers the active power loss of the resistance of earth line when one pole of the HVDC transmission line is under maintenance while the other pole is operating under monopolar ground circuit. Additionally, it considers the constraints when one converter station is under maintenance while the other converter station of the same type is under normal operation in VSC-MTDC transmission system.

2) The generalized Benders decomposition (GBD) algorithm is used to decompose the proposed COPD-MS model into the master problem of maintenance scheduling and the sub-problems of power distribution scheduling for iterative solution. For the sub-problems, the convex relaxation techniques and parallel computing technology are adopted to ensure the reliable convergence and improve the computational efficiency. For the master problem, the recursive acceleration (RA) algorithm is proposed, which can further improve the computational efficiency.

The rest of this paper is organized as follows. The formulation of the COPD-MS problem in an AC/DC power system is proposed in Section II. The GBD-RA algorithm for solving the proposed COPD-MS model efficiently is discussed in Section III. Case studies on the modified IEEE 39-bus system and an actual 1524-bus large-scale AC/DC hybrid power system are provided in Section IV. Section V gives the conclusion.

II. Problem Formulation

In a large-scale AC/DC power system, electric energy is transmitted from the sending area to the receiving area through AC, line-commutated converter based HVDC (LCC-HVDC), and VSC-MTDC transmission channels, as shown in Fig. 1. Under the condition that the total power transmission schedules of transmission sections and the active power output schedules of generators are known, formulating the power distribution schedules of multiple transmission channels can effectively reduce the active power loss of the transmission lines in the multiple paralleled AC/DC transmission channels. Meanwhile, to ensure the secure and reliable operation, each transmission channel needs regular preventive maintenance. Therefore, to coordinately formulate the power

distribution and maintenance schedules of the multiple paralleled transmission channels, a COPD-MS model is proposed below.

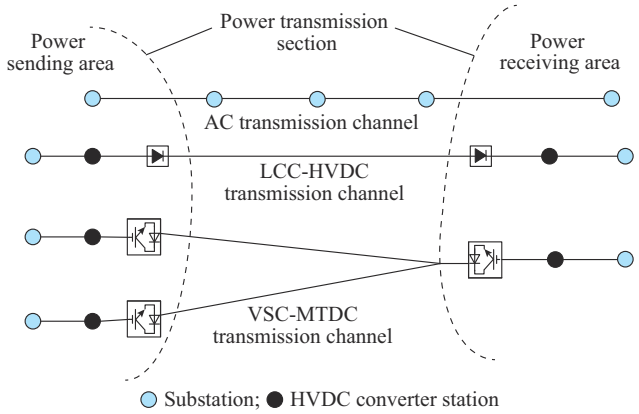

Fig. 1. Structure diagram of AC/DC power system.

A. Objective Function

The objective function of the proposed COPD-MS model of an AC/DC power system is the sum of the total active power loss cost of transmission lines and their maintenance cost, as shown in (1). For the schedule period of one month, assume that $\Delta T = 1$ hour, then $T = 720$ or 744 hours.

$$\min \sum_{t=1}^{T}\left[c_{g,t}\left(\sum_{k=1}^{N_{ac}} \Delta P_{Lak,t} + \sum_{l=1}^{N_{dc}} \Delta P_{Ldl,t} \right) + \sum_{m \in \Omega_m} c_{m,t} x_{m,t} \right] \Delta T \quad (1)$$

where $x_{m,t} = 1$ or $x_{m,t} = 0$ means that the transmission line m is under maintenance or normal operation at time t, respectively.

During the maintenance of an AC transmission line, its conductance and susceptance are both 0, as shown in (2). Meanwhile, the power loss of this line is also 0. Thus, $\Delta P_{Lak,t}$ in (1) can be expressed as (3).

$$\begin{cases} g'_{ak,t} = (1 - x_{m,t}) g_{ak} \\ b'_{ak,t} = (1 - x_{m,t}) b_{ak} \end{cases} \quad (2)$$

$$\Delta P_{Lak,t} = (V_{i,t}^2 + V_{j,t}^2 - 2V_{i,t}V_{j,t}\cos\theta_{ij,t}) g'_{ak,t} \quad (3)$$

In the actual AC/DC power system, most of the DC transmission lines are bipolar connections. Under the normal operation, a bipolar operation mode is used. However, the simultaneous maintenance of both poles of the HVDC transmission line has a significant impact on the secure operation of the AC/DC transmission systems. Thus, it is necessary to consider the situation where one pole of the HVDC transmission line is under maintenance while the other pole is operating under monopolar ground circuit, as shown in Fig. 2. This is a key difference between the maintenance of HVDC transmission lines and that of the AC transmission lines [24]. For the HVDC transmission line that is under maintenance, it includes two binary variables $x_{m_1,t}$ and $x_{m_2,t}$, which indicate whether the two poles of the HVDC transmission line are under maintenance, respectively, and m_1 and m_2 are two elements in the set of transmission lines under maintenance Ω_m. This means the two poles of an HVDC transmission line are deemed as two transmission lines in the proposed COPD-MS model. When the HVDC transmission line is operating as monopolar ground circuit, the active power loss of the resistance of earth line should be taken into account. When two poles of an HVDC transmission line are under maintenance simultaneously, this line is in the shutdown state, and the active power loss of this line is 0. Thus, $\Delta P_{Ldl,t}$ in (1) can be expressed as:

$$\Delta P_{Ldl,t} = K_{pl,t} I_{dl,t}^2 [R_{dl} + (2 - K_{pl,t}) R_{gl}] \quad (4)$$

$$K_{pl,t} = (1 - x_{m_1,t}) + (1 - x_{m_2,t}) \quad (5)$$

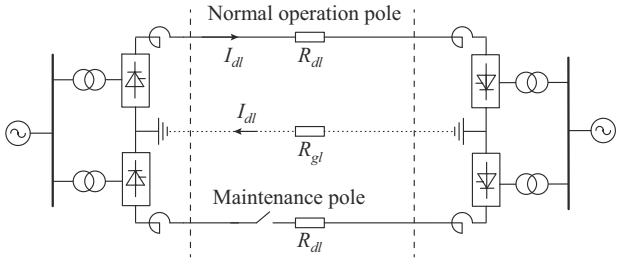

Fig. 2. Structure of HVDC transmission system.

B. Constraints

1) Constraints of Inter-area Power Transmission Schedule

The power transmission schedule constraint refers to the constraint of the total transmission power of the transmission sections between different areas, as shown in (6).

$$-\eta\% \cdot P_{\Sigma r,t} \le \sum_{k \in \Omega_{ar}} P_{ak,t} + \sum_{l \in \Omega_{dr}} P_{dl,t} - P_{\Sigma r,t} \le \eta\% \cdot P_{\Sigma r,t} \quad (6)$$

In (6), the transmission power of AC transmission line k $P_{ak,t}$ is expressed as (7), while the transmission power of DC transmission line l $P_{dl,t}$ is expressed as (8).

$$P_{ak,t} = V_{i,t}V_{j,t}(g'_{ak,t}\cos\theta_{ij,t} + b'_{ak,t}\sin\theta_{ij,t}) - V_{i,t}^2 g'_{ak,t} \quad (7)$$

$$P_{dl,t} = K_{pl,t} U_{di,t} I_{dl,t} \quad (8)$$

2) Constraints for Maintenance of Transmission Line

All transmission lines scheduled for maintenance must begin maintenance within their allowable earliest and latest start time. Also, these lines should be out of service during the time period for maintenance and operate normally during other periods. Assuming that the maintenance schedule of each transmission line should be during the dispatch period, the corresponding maintenance constraints are shown in (9).

$$\begin{cases} \sum_{t=T_{sm,\min}}^{T_{sm,\max}} s_{m,t} = 1 \\ x_{m,t} \le \sum_{t_1=1}^{t} s_{m,t_1} \\ \sum_{t_1=1}^{t+T_{mR}-1} x_{m,t_1} \ge T_{mR} s_{m,t} \\ \sum_{t=1}^{T} x_{m,t} = T_{mR} \end{cases} \quad (9)$$

where the 1st constraint indicates that the transmission lines need to start maintenance within the given time ranges; the 2nd constraint indicates that the binary variable $x_{m,t}$ must be 0

before the maintenance starts; and the 3rd and 4th constraints indicate that the binary variable $x_{m,t}$ must be 1 during all time periods for maintenance after the maintenance starts.

Due to the limited resources available for maintenance of transmission lines, it is impossible to maintain multiple transmission lines at the same time. Therefore, the number of transmission lines under maintenance should be less than a set value, as given in (10).

$$\sum_{m \in \Omega_m} x_{m,t} \le M_{\max} \tag{10}$$

Considering the operation flexibility of the VSC-MTDC transmission system, when the DC transmission line connected to one converter station is under maintenance, the DC transmission lines connected to the other converter stations can still operate. Taking the "Kun-Liu-Long" VSC-MTDC system (denoted as VSC(Kun-Liu-Long)) as an example, there is one rectifier station and two inverter stations, as shown in Fig. 3. When the DC transmission line connected to the rectifier station is under bipolar maintenance, the entire VSC-MTDC transmission system is out of service. When the DC transmission line connected to the rectifier station is under monopolar maintenance, the corresponding poles of both inverter stations cannot operate. When the DC transmission line connected to one inverter station is under monopolar or bipolar maintenance, the rectifier station and the other inverter station can still operate normally. The corresponding constraints are shown in (11).

$$\begin{cases} \sum_{m \in \Omega_R} x_{m,t} \ge \sum_{m \in \Omega_{I_1}} x_{m,t} \\ \sum_{m \in \Omega_R} x_{m,t} \ge \sum_{m \in \Omega_{I_2}} x_{m,t} \end{cases} \tag{11}$$

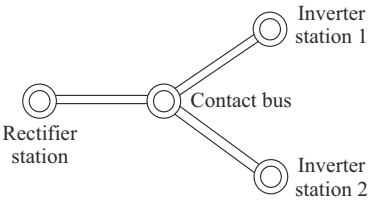

Fig. 3. Structure diagram of VSC(Kun-Liu-Long) system.

3) Constraints of DC System Operation

For the LCC-HVDC transmission lines, considering the influence of the converter transformer regulation and commutation reactance [25], the operation constraints are given as:

$$\begin{cases} U_{di,t} = \dfrac{3\sqrt{2}}{\pi} K_{di} V_{i,t} \cos\psi_{i,t} - \dfrac{3}{\pi} X_{ci} I_{di,t} \\ U_{di,t} = \dfrac{3\sqrt{2}}{\pi} K_{di} V_{i,t} \cos\varphi_{i,t} \\ P_{di,t} = K_{pl,t} U_{di,t} I_{di,t} \\ Q_{di,t} = K_{pl,t} U_{di,t} I_{di,t} \tan\varphi_{i,t} \\ U_{diR,t} = U_{diI,t} + I_{di,t} R_{dl} \end{cases} \tag{12}$$

where the 1st constraint reflects the relationship between the current and voltage of the converter station; and the 2nd constraint reflects the relationship between the AC voltage and DC voltage of the converter station. Note that the subscripts R and I represent the rectifier and inverter stations, respectively.

For the VSC-MTDC transmission lines, considering the impact of the equivalent resistance of the VSC-MTDC converter station [26], the operation constraints after eliminating the connecting buses of the DC system are given as:

$$\begin{cases} P_{vi,t} - \dfrac{\mu_i M_{i,t}}{\sqrt{2}} V_{i,t} U_{vi,t} Y_i \sin\delta_{i,t} = 0 \\ Q_{vi,t} + \dfrac{\mu_i M_{i,t}}{\sqrt{2}} V_{i,t} U_{vi,t} Y_i \cos\delta_{i,t} - V_{i,t}^2 Y_i = 0 \\ P_{vi,t} = K_{pi,t} U_{vi,t} I_{vi,t} \\ I_{vi,t} = \sum_{j=1, j\ne i}^{N_v} I_{vij,t} \\ I_{vij,t} = \dfrac{U_{vi,t} - U_{vj,t}}{R_{vij}} \end{cases} \tag{13}$$

4) Constraints of AC System Operation

Considering the maintenance of AC transmission lines, it is necessary to modify the relevant elements in the nodal admittance matrix, i.e., Y_{ii}, Y_{ij}, Y_{ji}, and Y_{jj}, associated with the buses i and j of the maintained lines, as shown in (14).

$$\begin{cases} Y_{ii} = Y_{ii}^0 - x_{m,t}(y_{ij} + \mathrm{j}B_{ij}/2) \\ Y_{jj} = Y_{jj}^0 - x_{m,t}(y_{ij} + \mathrm{j}B_{ij}/2) \\ Y_{ij} = Y_{ji} = Y_{ij}^0 + x_{m,t} y_{ij} \end{cases} \tag{14}$$

After modifying the nodal admittance matrix, the power balance equations for AC buses that are not connected to an HVDC converter station, an LCC-HVDC converter station, or a VSC-MTDC converter station are shown in (15)-(17), respectively. In (16), the sign ± is negative or positive for a rectifier or inverter station, respectively.

$$\begin{cases} P_{Gi,t} - P_{Li,t} - V_{i,t} \sum_{j=1}^{N} V_{j,t} (G_{ij} \cos\theta_{ij,t} + B_{ij} \sin\theta_{ij,t}) = 0 \\ Q_{Gi,t} - Q_{Li,t} - V_{i,t} \sum_{j=1}^{N} V_{j,t} (G_{ij} \sin\theta_{ij,t} - B_{ij} \cos\theta_{ij,t}) = 0 \end{cases} \tag{15}$$

$$\begin{cases} -V_{i,t} \sum_{j=1}^{N} V_{j,t} (G_{ij} \cos\theta_{ij,t} + B_{ij} \sin\theta_{ij,t}) \pm P_{di,t} = 0 \\ -V_{i,t} \sum_{j=1}^{N} V_{j,t} (G_{ij} \sin\theta_{ij,t} - B_{ij} \cos\theta_{ij,t}) - Q_{di,t} = 0 \end{cases} \tag{16}$$

$$\begin{cases} -V_{i,t} \sum_{j=1}^{N} V_{j,t} (G_{ij} \cos\theta_{ij,t} + B_{ij} \sin\theta_{ij,t}) - P_{vi,t} = 0 \\ -V_{i,t} \sum_{j=1}^{N} V_{j,t} (G_{ij} \sin\theta_{ij,t} - B_{ij} \cos\theta_{ij,t}) - Q_{vi,t} = 0 \end{cases} \tag{17}$$

5) Constraints for Upper Bound (UB) and Lower Bound (LB) of Variables

The constraints for UB and LB of variables include AC bus voltage amplitude, DC voltage and current, transmission power of each channel, control angle of LCC-HVDC converter station, modulation ratio of VSC-MTDC converter sta-

tion, and active and reactive power outputs of the swing generators, as shown in (18).

$$\boldsymbol{h}_{\min} \le \boldsymbol{h} \le \boldsymbol{h}_{\max} \tag{18}$$

where $\boldsymbol{h}=[V_{i,t}, U_{di,t}, I_{di,t}, U_{vi,t}, I_{vi,t}, P_{ak,t}, P_{dl,t}, \psi_{i,t}, M_{i,t}, P_{Gs,t}, Q_{Gs,t}]$.

In summary, (1)-(18) constitute the proposed COPD-MS model of multiple paralleled transmission channels in an AC/DC power system. This model is a mixed-integer nonlinear programming (MINLP) model, which is difficult to solve directly. Therefore, based on the GBD algorithm, an efficient algorithm for solving the proposed COPD-MS model is proposed.

III. Model Solution

A. GBD Algorithm

The Benders decomposition algorithm was first proposed by J. F. Benders in 1962, A. M. Geoffrion extended the Benders decomposition algorithm to MINLP problems and proposed the GBD algorithm [27]. The algorithmic theory is similar to the Benders decomposition algorithm, but the sub-problem is not necessarily a linear programming. To facilitate the description, the proposed COPD-MS model described in (1)-(18) can be written in a compact form as:

$$\begin{cases} \min\limits_{\boldsymbol{X},\boldsymbol{Y}} f(\boldsymbol{X},\boldsymbol{Y}) \\ \text{s.t. } \boldsymbol{G}_1(\boldsymbol{X})=\boldsymbol{0} \\ \quad \boldsymbol{G}_2(\boldsymbol{X},\boldsymbol{Y})=\boldsymbol{0} \\ \quad \boldsymbol{H}_1(\boldsymbol{X})\le\boldsymbol{0} \\ \quad \boldsymbol{H}_2(\boldsymbol{X},\boldsymbol{Y})\le\boldsymbol{0} \end{cases} \tag{19}$$

where $\boldsymbol{X}$ represents binary variables related to maintenance, which includes $x_{m,t}$ and $s_{m,t}$; $\boldsymbol{Y}$ represents continuous variables, which includes $P_{ak,t}$, $P_{dl,t}$, $\Delta P_{Lak,t}$, $\Delta P_{Ldl,t}$, $V_{i,t}$, $\theta_{ij,t}$, $U_{di,t}$, $I_{di,t}$, $\varphi_{i,t}$, $M_{i,t}$, $U_{vi,t}$, I_{vi}, $\delta_{i,t}$, $P_{di,t}$, $Q_{di,t}$, $P_{vi,t}$, $Q_{vi,t}$, $P_{Gs,t}$, and $Q_{Gs,t}$; $\boldsymbol{G}_1(\boldsymbol{X})$ and $\boldsymbol{H}_1(\boldsymbol{X})$ represent the equality and inequality constraints that only involve binary variables as given in (9)-(11), respectively; and $\boldsymbol{G}_2(\boldsymbol{X},\boldsymbol{Y})$ and $\boldsymbol{H}_2(\boldsymbol{X},\boldsymbol{Y})$ represent the remaining equality and inequality constraints, respectively, as given in (2)-(8) and (12)-(18).

Formula (19) is the original problem, which is then decomposed into the master problem and the sub-problems. The master problem only contains binary variables that describe maintenance, and its constraints include the maintenance constraints (9)-(11) and the added Benders cuts after solving the sub-problems, as shown in (20). The master problem is a 0-1 integer programming, which is a relaxation problem of the original problem, and its optimal value is the LB of the optimal values of the original problem (19). By solving the master problem, the value of the maintenance variables can be obtained and transmitted to the sub-problems.

$$\begin{cases} \min\limits_{\boldsymbol{X}} \alpha \\ \text{s.t. } \boldsymbol{G}_1(\boldsymbol{X})=\boldsymbol{0} \\ \quad \boldsymbol{H}_1(\boldsymbol{X})\le\boldsymbol{0} \\ \quad \text{Benders cuts} \end{cases} \tag{20}$$

where α is the value of LB of the original problem.

When the maintenance schedules are determined, the sub-problems are continuous nonlinear programming, as shown in (21). The optimal value is the UB of the optimal value of the original problem (19).

$$\begin{cases} \min\limits_{\boldsymbol{Y}} f(\boldsymbol{X},\boldsymbol{Y}) \\ \text{s.t. } \boldsymbol{G}_2(\boldsymbol{X},\boldsymbol{Y})=\boldsymbol{0} \\ \quad \boldsymbol{H}_2(\boldsymbol{X},\boldsymbol{Y})\le\boldsymbol{0} \\ \quad \boldsymbol{X}=\boldsymbol{X}^{(k)}: \boldsymbol{\lambda}^{(k)} \end{cases} \tag{21}$$

where $\boldsymbol{\lambda}^{(k)}$ represent the dual variables obtained by solving sub-problems in the k^{th} iteration.

The added Benders cut in the master problem (20) after solving the sub-problems for the k^{th} iteration is shown in (22). In fact, since the master problem provides the values of maintenance variables, the sub-problem is a multi-period optimization for power distribution (OPD) problem. Since there is no coupling among OPD during each time interval in the sub-problem, the parallel computing technology is used to improve the computational efficiency of the model solution.

$$\alpha \ge f(\boldsymbol{X}^{(k)}, \boldsymbol{Y}^{(k)}) + \sum (\boldsymbol{\lambda}^{(k)})^{\mathrm{T}} (\boldsymbol{X}-\boldsymbol{X}^{(k)}) \tag{22}$$

The diagram of using the GBD algorithm to solve the proposed COPD-MS model is shown in Fig. 4, where λ_m is the elements of $\boldsymbol{\lambda}$.

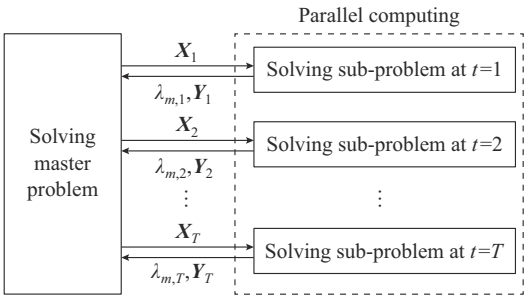

Fig. 4. Alternative iteration between master problem and sub-problems.

B. Convex Relaxation of Sub-problems

When the GBD algorithm is used and the sub-problem is non-convex, there exist dual gaps and the sub-problem cannot converge to the optimal solution of the original problem [28]. Therefore, to ensure the reliable convergence, the convex relaxation techniques are applied to relax the non-convex constraints in the sub-problems into convex ones.

1) Convex Relaxation of AC System

The non-convex constraints of AC system include (3), (7), and (15)-(17), which can adopt the second-order cone (SOC) relaxation method [29]. By introducing the variables $R_{ij,t}=V_{i,t}V_{j,t}\cos\theta_{ij,t}$, $T_{ij,t}=V_{i,t}V_{j,t}\sin\theta_{ij,t}$, and $U_{i,t}=V_{i,t}^2$, (3), (7), and (15) can be written as (23)-(25), respectively. Moreover, (16) and (17) can also be convex relaxed using the same method.

$$\Delta P_{Lak,t}=(U_{i,t}+U_{j,t}-2R_{ij,t})g'_{ak,t} \tag{23}$$

$$P_{ak,t}=R_{ij,t}g'_{ak,t}+T_{ij,t}b_{ak,t}-U_{i,t}g'_{ak,t} \tag{24}$$

$$\begin{cases} P_{Gi,t}-P_{Li,t}-U_{i,t}G_{ii}-\sum\limits_{j=1,j\neq i}^{N}(R_{ij,t}G_{ij}+T_{ij,t}B_{ij})=0 \\ Q_{Gi,t}-Q_{Li,t}+U_{i,t}B_{ii}-\sum\limits_{j=1,j\neq i}^{N}(T_{ij,t}G_{ij}-R_{ij,t}B_{ij})=0 \\ \left\| 2R_{ij,t} \quad 2T_{ij,t} \quad U_{i,t}-U_{j,t} \right\|_2-(U_{i,t}+U_{j,t})\le 0 \\ R_{ij,t}-R_{ji,t}=0 \\ T_{ij,t}+T_{ji,t}=0 \\ \sum\limits_{ij\in\Omega_k}\left[\arctan\dfrac{T^0_{ij,t}}{R^0_{ij,t}}+\dfrac{R^0_{ij,t}T_{ij,t}-T^0_{ij,t}R_{ij,t}}{(R^0_{ij,t})^2+(T^0_{ij,t})^2}\right]=0 \end{cases} \tag{25}$$

2) Convex Relaxation of DC System

The non-convex constraints of DC systems include (8), (12), and (13). By combining the 2nd and 5th constraints in (12) for the LCC-HVDC converter stations, (26) can be obtained. By introducing the variables $\tilde{I}_{di,t}=I^2_{di,t}$ and the constant $K_i=(3\sqrt{2}/\pi)K_{pl,t}K_{di}$, the 1st and 2nd equations in (26) can be written as (27) by using the SOC relaxation method. By introducing the variables $\tilde{U}_{di,t}=U^2_{di,t}$ and the two sides of the 5th equation in (26) are multiplied by $K_{pl,t}(U_{diR,t}+U_{diL,t})$, other equations in (26) can be written as (28).

$$\begin{cases} P_{di,t}=\dfrac{3\sqrt{2}}{\pi}K_{pl,t}K_{di}V_{i,t}I_{di,t}\cos\varphi_{i,t} \\ Q_{di,t}=\dfrac{3\sqrt{2}}{\pi}K_{pl,t}K_{di}V_{i,t}I_{di,t}\sin\varphi_{i,t} \\ P_{diR,t}=K_{pl,t}U_{diR,t}I_{di,t} \\ P_{diL,t}=P_{diR,t}-K_{pl,t}I^2_{di,t}R_{dl} \\ U_{diR,t}-U_{diL,t}=I_{di,t}R_{dl} \end{cases} \tag{26}$$

$$\left\| 2P_{di,t} \quad 2Q_{di,t} \quad K_i(\tilde{I}_{di,t}-U_{i,t}) \right\|_2-K_i(\tilde{I}_{di,t}+U_{i,t})\le 0 \tag{27}$$

$$\begin{cases} \left\| 2P_{diR,t} \quad K_{pl,t}(\tilde{I}_{di,t}-\tilde{U}_{diR,t}) \right\|_2-K_{pl,t}(\tilde{I}_{di,t}+\tilde{U}_{diR,t})\le 0 \\ P_{diL,t}=P_{diR,t}-K_{pl,t}\tilde{I}_{di,t}R_{dl} \\ K_{pl,t}(\tilde{U}_{diR,t}-\tilde{U}_{diL,t})=(P_{diR,t}+P_{diL,t})R_{dl} \end{cases} \tag{28}$$

Square both sides of the first constraint in (12) after moving terms, (29) can be obtained. By introducing variables $\Phi_{i,t}=\cos^2\psi_{i,t}$ and $w_{i,t}=U_{i,t}\Phi_{i,t}$, (29) can be written as (30) by the McCormick convex envelope relaxation method [30].

$$\tilde{U}_{di,t}+\frac{6}{\pi}X_{ci}P_{di,t}+\left(\frac{3}{\pi}X_{ci}\right)^2\tilde{I}_{di,t}=\left(\frac{3\sqrt{2}}{\pi}K_{di}\right)^2U_{i,t}\cos^2\psi_{i,t} \tag{29}$$

$$\begin{cases} \tilde{U}_{di,t}+\dfrac{6}{\pi}X_{ci}P_{di,t}+\left(\dfrac{3}{\pi}X_{ci}\right)^2\tilde{I}_{di,t}=\left(\dfrac{3\sqrt{2}}{\pi}K_{di}\right)^2w_{i,t} \\ U_{i,\min}\Phi_{i,t}+\Phi_{i,\min}U_{i,t}-U_{i,\min}\Phi_{i,\min}-w_{i,t}\le 0 \\ U_{i,\max}\Phi_{i,t}+\Phi_{i,\max}U_{i,t}-U_{i,\max}\Phi_{i,\max}-w_{i,t}\le 0 \\ w_{i,t}-U_{i,\min}\Phi_{i,t}-\Phi_{i,\max}U_{i,t}+U_{i,\min}\Phi_{i,\max}\le 0 \\ w_{i,t}-U_{i,\max}\Phi_{i,t}-\Phi_{i,\min}U_{i,t}+U_{i,\max}\Phi_{i,\min}\le 0 \end{cases} \tag{30}$$

For the constraint (8) of transmission power of DC transmission line, it can also be written as the similar form of the first inequation in (28) by SOC relaxation method.

By combining the 3rd-5th constraints in (13) for VSC-MTDC converter stations, (31) can be obtained. By introducing the variables $\tilde{I}_{vi,t}=I^2_{vi,t}$ and $\tilde{U}_{vi,t}=U^2_{vi,t}$, (31) can be written as (32) through the SOC relaxation method.

$$\begin{cases} P_{vi,t}=\sum\limits_{j=1,j\neq i}^{N_v}P_{vij,t} \\ P_{vi,t}=K_{pl,t}U_{vi,t}I_{vi,t} \\ P_{vij,t}-P_{vji,t}=I^2_{vij,t}R_{vij} \\ U_{vi,t}-U_{vj,t}=I_{vij,t}R_{vij} \end{cases} \tag{31}$$

$$\begin{cases} P_{vi,t}=\sum\limits_{j=1,j\neq i}^{N_v}P_{vij,t} \\ \left\| 2P_{vij,t} \quad K_{pl,t}(\tilde{I}_{vij,t}-\tilde{U}_{vij,t}) \right\|_2-K_{pl,t}(\tilde{I}_{vij,t}+\tilde{U}_{vij,t})\le 0 \\ P_{vij,t}-P_{vji,t}=\tilde{I}_{vij,t}R_{vij} \\ \tilde{U}_{vi,t}-\tilde{U}_{vj,t}=(P_{vij,t}+P_{vji,t})R_{vij} \end{cases} \tag{32}$$

Assuming that $K_{vi,t}=M_{i,t}V_{i,t}U_{vi,t}\sin\delta_{i,t}$, $L_{vi,t}=M_{i,t}V_{i,t}U_{vi,t}\cdot\cos\delta_{i,t}$, $\tilde{M}_{i,t}=M^2_{i,t}$, $\tilde{U}_{vi,t}=U^2_{vi,t}$, and $Z_{i,t}=\tilde{M}_{i,t}\tilde{U}_{vi,t}$, the 1st and 2nd equations in (10) can be transformed into the convex constraints as:

$$\begin{cases} P_{vi,t}-\dfrac{\mu_i}{\sqrt{2}}Y_iK_{vi,t}=0 \\ Q_{vi,t}+\dfrac{\mu_i}{\sqrt{2}}Y_iL_{vi,t}-U_{i,t}Y_i=0 \\ \left\| 2K_{vi,t} \quad 2L_{vi,t} \quad Z_{i,t}-U_{i,t} \right\|_2\le Z_{i,t}+U_{i,t} \\ \tilde{U}_{vi,\min}\tilde{M}_{i,t}+\tilde{M}_{i,\min}\tilde{U}_{vi,t}-\tilde{U}_{vi,\min}\tilde{M}_{i,\min}-Z_{i,t}\le 0 \\ \tilde{U}_{vi,\max}\tilde{M}_{i,t}+\tilde{M}_{i,\max}\tilde{U}_{vi,t}-\tilde{U}_{vi,\max}\tilde{M}_{i,\max}-Z_{i,t}\le 0 \\ Z_{i,t}-\tilde{U}_{vi,\min}\tilde{M}_{i,t}-\tilde{M}_{i,\max}\tilde{U}_{vi,t}+\tilde{U}_{vi,\min}\tilde{M}_{i,\max}\le 0 \\ Z_{i,t}-\tilde{U}_{vi,\max}\tilde{M}_{i,t}-\tilde{M}_{i,\min}\tilde{U}_{vi,t}+\tilde{U}_{vi,\max}\tilde{M}_{i,\min}\le 0 \end{cases} \tag{33}$$

C. RA Algorithm for Solving Master Problem

By using the GBD algorithm, the original large-scale MINLP problem has been converted to iteratively solving the linear 0-1 programming master problem and the SOC programming sub-problems. Both of them have smaller scale and lower computational complexity, which can be solved by the mature commercial solver GUROBI. However, the master problem still requires lots of computational time to solve because many 0-1 variables are included. Therefore, the RA algorithm is proposed to improve the computational efficiency.

After k iterations, the master problem to be solved in the $(k+1)^{\text{th}}$ iteration is shown in (34), which only adds a new Benders cut constraint compared with the master problem solved in the k^{th} iteration. It is obvious that the solution $\boldsymbol{X}^{(k)}$ obtained by solving the master problem in the k^{th} iteration satisfies all the constraints in (34) except for the added Benders cut constraint. Thus, a method to efficiently obtain the solution of the $(k+1)^{\text{th}}$ master problem from $\boldsymbol{X}^{(k)}$ is required. By combining the characteristics of 0-1 programming and

the added Benders cut constraint, the RA algorithm is adopted.

$$\begin{cases} \min\limits_{X} \alpha \\ \text{s.t. } \boldsymbol{G}_1(\boldsymbol{X})=\boldsymbol{0} \\ \quad \boldsymbol{H}_1(\boldsymbol{X})\le \boldsymbol{0} \\ \quad \alpha \ge f(\boldsymbol{X}^{(1)},\boldsymbol{Y}^{(1)})+\sum(\boldsymbol{\lambda}^{(1)})^{\mathrm{T}}(\boldsymbol{X}-\boldsymbol{X}^{(1)}) \\ \quad \vdots \\ \quad \alpha \ge f(\boldsymbol{X}^{(k)},\boldsymbol{Y}^{(k)})+\sum(\boldsymbol{\lambda}^{(k)})^{\mathrm{T}}(\boldsymbol{X}-\boldsymbol{X}^{(k)}) \end{cases} \tag{34}$$

In (34), the objective function is to minimize the value of α. Therefore, the added Benders cut constraint needs to keep the value of α as small as possible. Due to the fact that the 1st term $f(\boldsymbol{X}^{(k)},\boldsymbol{Y}^{(k)})$ in the added Benders cut constraint is a constant value, it is necessary to search $\boldsymbol{X}$ to minimize the value of the 2nd term $\sum(\boldsymbol{\lambda}^{(k)})^{\mathrm{T}}(\boldsymbol{X}-\boldsymbol{X}^{(k)})$. Considering that this is a 0-1 programming problem, the elements in $\boldsymbol{X}$ can only be 0 or 1. For convenience, compared with the solution $\boldsymbol{X}^{(k)}$, if the corresponding element in $\boldsymbol{X}$ changes, it is called an inversion. Thus, the value of $(\boldsymbol{\lambda}^{(k)})^{\mathrm{T}}(\boldsymbol{X}-\boldsymbol{X}^{(k)})$ is shown in Table I. Therefore, whether the elements in $\boldsymbol{X}$ are inversed depends on the values of $\boldsymbol{\lambda}^{(k)}$ and $\boldsymbol{X}^{(k)}$. It can be observed from Table I that, to minimize the value of $(\boldsymbol{\lambda}^{(k)})^{\mathrm{T}}(\boldsymbol{X}-\boldsymbol{X}^{(k)})$, the elements in $\boldsymbol{X}$ need to be inversed when $\boldsymbol{\lambda}^{(k)}>\boldsymbol{0}$ and $\boldsymbol{X}^{(k)}=\boldsymbol{1}$, or $\boldsymbol{\lambda}^{(k)}<\boldsymbol{0}$ and $\boldsymbol{X}^{(k)}=\boldsymbol{0}$.

TABLE I
VALUE OF $(\boldsymbol{\lambda}^{(k)})^{\mathrm{T}}(\boldsymbol{X}-\boldsymbol{X}^{(k)})$

State	$(\boldsymbol{\lambda}^{(k)})^{\mathrm{T}}(\boldsymbol{X}-\boldsymbol{X}^{(k)})$	
	$\boldsymbol{X}^{(k)}=\boldsymbol{0}$	$\boldsymbol{X}^{(k)}=\boldsymbol{1}$
Inversed	$\boldsymbol{\lambda}^{(k)}$	$-\boldsymbol{\lambda}^{(k)}$
Not inversed	$\boldsymbol{0}$	$\boldsymbol{0}$

Whether all elements in $\boldsymbol{X}$ are inversed or not based on the values of $\boldsymbol{\lambda}^{(k)}$ and $\boldsymbol{X}^{(k)}$, the value of $(\boldsymbol{\lambda}^{(k)})^{\mathrm{T}}(\boldsymbol{X}-\boldsymbol{X}^{(k)})$ can be kept as small as possible. However, the solution obtained by this way often does not satisfy the maintenance constraints in (34) because the maintenance schedules need to have temporal continuity. In the proposed COPD-MS model, $\boldsymbol{X}$ includes variables $s_{m,t}$ for describing whether the line maintenance starts and $x_{m,t}$ for describing whether the line is under maintenance. In fact, the values of these two variables are directly related, and the value of $x_{m,t}$ can be determined by $s_{m,t}$ according to (11). Therefore, it is only necessary to determine whether the variable $s_{m,t}$ needs to be inversed. Since the transmission lines only need maintenance once in the schedule period, in order to minimize the value of $\sum(\boldsymbol{\lambda}^{(k)})^{\mathrm{T}}(\boldsymbol{X}-\boldsymbol{X}^{(k)})$, it is necessary to inverse $s_{m,t}$ corresponding to the larger absolute values in the elements of $\boldsymbol{\lambda}^{(k)}$. The pseudocode of the RA algorithm is shown in Algorithm 1.

In summary, the flowchart of the GBD-RA algorithm is shown in Fig. 5. By using the RA algorithm for solving the master problem of each iteration, a new solution is obtained without solving the large-scale master problem each time, which can significantly improve the computational efficiency.

Algorithm 1: RA algorithm for solving master problem

Step 1: transmit the solution of the master problem in the k^{th} iteration to the sub-problem, and obtain $\boldsymbol{\lambda}^{(k)}$.

Step 2: order the elements of $\boldsymbol{\lambda}^{(k)}$ according to the absolute values, and determine whether $s_{m,t}$ needs to be inversed based on the values of $\boldsymbol{\lambda}^{(k)}$ and $\boldsymbol{X}^{(k)}$.

Step 3: obtain $x_{m,t}$ directly based on the value of $s_{m,t}$ and the required maintenance time for each transmission line.

Step 4: verify whether the solution satisfies other $k-1$ Benders cut constraints and the constraint (12). If yes, go to *Step 5*; otherwise, go to *Step 6*.

Step 5: transmit the values of all maintenance variables to the sub-problem.

Step 6: use the solver GUROBI to directly solve the master problem that includes all constraints.

Step 7: end.

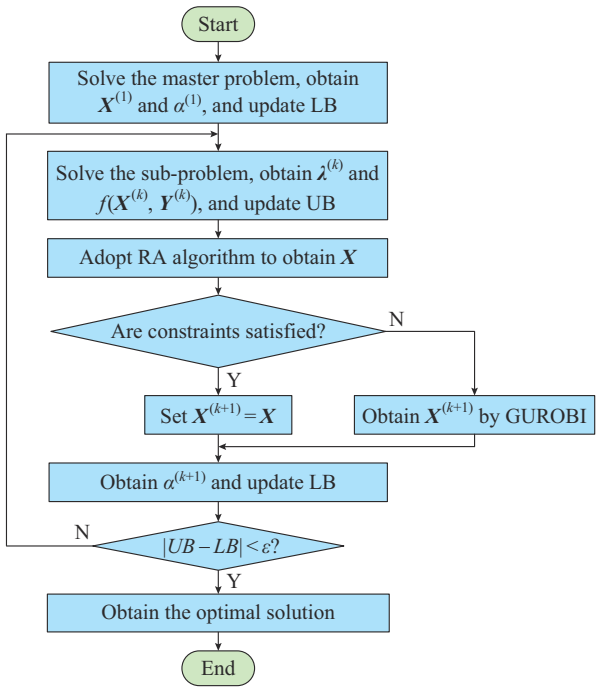

Fig. 5. Flowchart of GBD-RA algorithm.

IV. CASE STUDIES

The modified IEEE 39-bus system and an actual 1524-bus large-scale AC/DC hybrid power system are used to demonstrate the effectiveness of the proposed COPD-MS model. A PC with an Intel Core i7-9700 and 16 GB of RAM is used, and the computing platforms are MATLAB 2018b and GAMS 24.5.6. In the two case studies, the electricity price $c_{g,t}$ is set to be 0.37 ¥/kWh during 00:00-08:00, 1.06 ¥/kWh during 09:00-12:00 and 14:00-19:00, and 0.74 ¥/kWh during other time in a day. The allowable deviation of the power exchange η% is set to be 5%, and the maximum allowable number of maintenance lines $M_{\max}$ is set to be 4. The initial values of LB and UB are set to be 0, and the convergence accuracy ε is set to be 0.01.

A. Modified IEEE 39-bus System

The modified IEEE 39-bus system is divided into Area 1 and Area 2, as shown in Fig. 6. The multiple paralleled AC/

DC transmission channels between the two areas include the AC transmission lines 31-1, 14-15, and 22-21 (denoted as AC(31-1), AC(14-15), and AC(22-21), respectively), LCC-HVDC transmission line 4-3 (denoted as LCC(4-3)), and three-terminal VSC-MTDC transmission line 19-24-16 (denoted as VSC(19), VSC(24), VSC(16), respectively). Considering the monthly COPD-MS problem, all of the transmission lines need maintenance once during this month, and each pole of the HVDC transmission line needs maintenance.

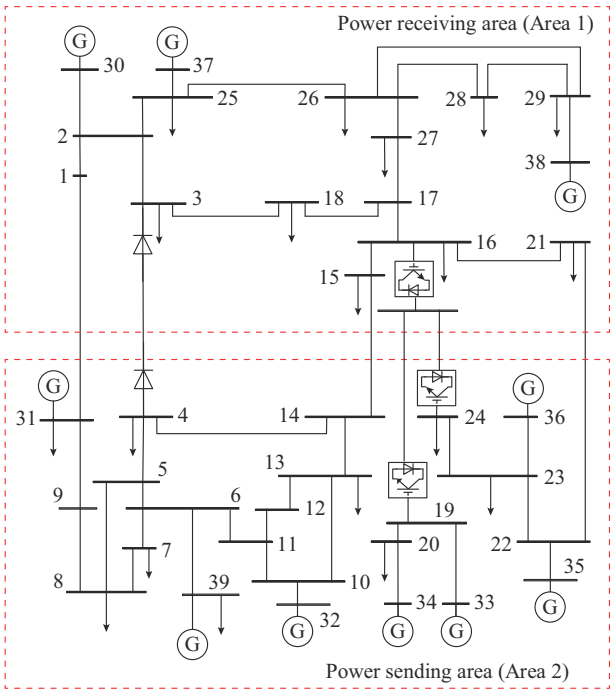

Fig. 6. Structure diagram of modified IEEE 39-bus system.

The data of transmission lines for maintenance is shown in Table II. The monthly power exchange schedule curve between the two areas is shown in Fig. 7.

TABLE II
DATA OF TRANSMISSION LINES FOR MAINTENANCE IN MODIFIED IEEE 39-BUS SYSTEM

Transmission line	$T_{sm,\min}$ (hour)	$T_{sm,\max}$ (hour)	T_{mR} (hour)	$c_{m,t}$ (10^3 ¥)		Rated power (MW)
				Weekday	Weekend	
AC(31-1)	49	241	72	1.1	1.5	6
AC(14-15)	125	317	72	1.2	1.6	3
AC(22-21)	385	553	72	1.4	1.9	5
LCC(4-3)	1	301	72×2	1.8	2.4	4
VSC(19)	361	649	96×2	2.0	2.5	4
VSC(24)	361	649	96×2	2.0	2.5	5
VSC(16)	361	649	96×2	2.0	2.5	9

1) Validity Analysis of Convex Relaxation of Sub-problem

To verify the computational accuracy of the convex relaxation, without considering the maintenance schedules, the solutions of the power distribution models without and with the convex relaxation at $t=1$ hour by using the commercial solvers CONOPT and GUROBI are shown in Table III.

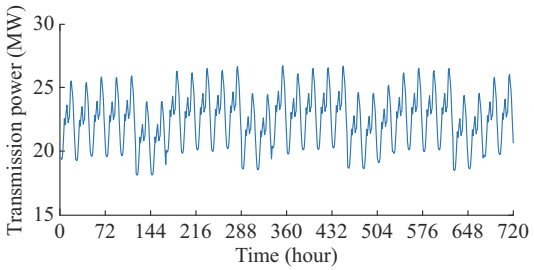

Fig. 7. Monthly power exchange schedule curve between two areas in modified IEEE 39-bus system.

TABLE III
SOLUTIONS OF POWER DISTRIBUTION MODEL WITHOUT AND WITH CONVEX RELAXATION AT $t=1$ HOUR

Model	Active power loss (MWh)	Relaxation gap		CPU time (s)
		Maximum	Average	
Without convex relaxation	0.82			2.23
With convex relaxation	0.83	4.83×10^{-2}	1.62×10^{-3}	1.06

It can be observed that the active power losses of the parallel AC/DC transmission channels are very close and the average relaxation gap is only at the order of magnitude of 10^{-3}, and the consumed CPU time is reduced by 52.4%, which demonstrates the high computational accuracy and efficiency of the convex relaxation method. Therefore, all subsequent calculations are based on the model with convex relaxation.

2) Solution of Proposed COPD-MS Model

The solution for the proposed COPD-MS model can simultaneously obtain the maintenance and power transmission schedules for transmission lines, as shown in Figs. 8 and 9, respectively.

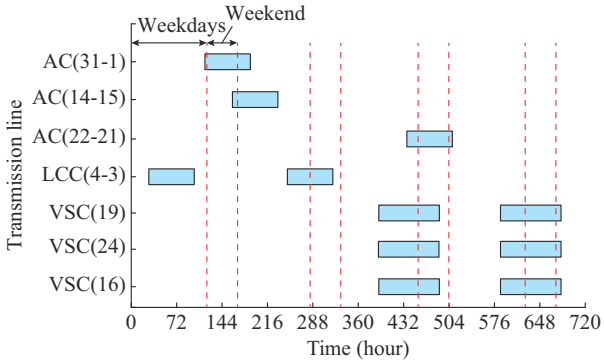

Fig. 8. Maintenance schedules of transmission lines in modified IEEE 39-bus system.

The blue rectangles corresponding to each transmission line in Fig. 8 represent the maintenance time. It can be observed that all transmission lines are scheduled for maintenance on weekends and the time close to weekends, because the load power and the transmission power on weekends are low. Formulating the maintenance schedule at this time can reduce the influence on the power exchange schedules. For the LCC-HVDC and VSC-MTDC transmission lines, the monopolar maintenance is adopted.

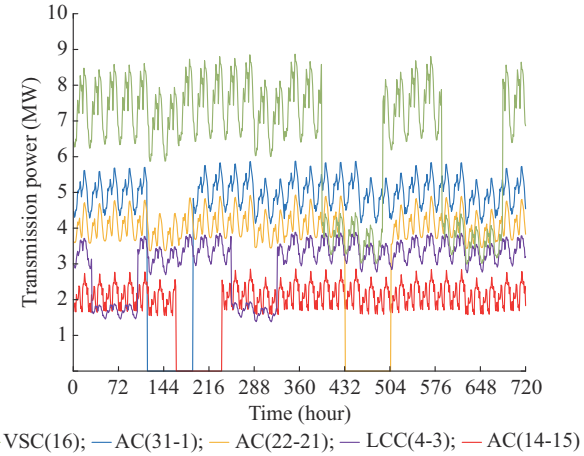

Fig. 9. Power transmission schedules of transmission lines in modified IEEE 39-bus system.

In addition, the monopolar maintenance time for three terminals of the VSC-MTDC transmission lines is the same. This is because when the HVDC transmission lines connected to the inverter station is under monopolar maintenance, the other two HVDC transmission lines connected to the two rectifier stations using monopolar maintenance simultaneously can avoid the impact of required subsequent maintenance tasks on completing the given power exchange schedule. In Fig. 8, the two maintenances of each DC transmission line (denoted by two blue rectanges) are the maintenance schedules of its two poles, respectively.

It can be observed from Fig. 9 that when the AC transmission line is under maintenance, its transmission power becomes 0; when the DC transmission line is under maintenance, it can still operate under the monopolar ground circuit, and its transmission power becomes approximately half of the original.

To illustrate the necessity of considering the monopolar maintenance, the results of the following two cases are given for comparison.

1) Case 1: considering monopolar maintenance, where one pole of an HVDC transmission line is under maintenance while the other pole is operating under monopolar ground circuit.

2) Case 2: without considering monopolar maintenance, where the two poles of an HVDC transmission line are under maintenance at the same time.

The comparative results of cases 1 and 2 are shown in Table IV. It can be observed that the proposed COPD-MS model considering monopolar maintenance (case 1) can effectively reduce the maintenance costs and transmission losses. This is because when one pole is under maintenance, the other pole can still transmit power normally, which can increase the number of transmission channels to be decided and reduce the influence of maintenance of HVDC transmission lines on the power transmission of the AC/DC power system.

3) Analysis of Effect of Coordinated Optimization

In the current AC/DC power system operation, the existing model firstly formulates the maintenance schedules of transmission lines and then formulates their power distribution schedules.

TABLE IV
COMPARATIVE RESULTS OF CASES 1 AND 2

Case No.	Objective value (10^4 ¥)	Maintenance cost (10^4 ¥)	Transmission loss (MWh)
1	147.91	99.81	717.85
2	158.62	106.94	742.36

To illustrate the effectiveness of the proposed COPD-MS model for power distribution and maintenance schedules, its results are compared with those of the existing model, as shown in Table V, where the starting maintenance time of each transmission line in Schedule 1 and Schedule 2 are taken as $T_{sm,\min}$ and $T_{sm,\max}$ given in Table II, respectively, and the constraints considered in formulating the power distribution schedule are consistent with those in the proposed COPD-MS model. It can be observed that the maintenance cost and total power loss obtained by the proposed COPD-MS model are both lower than those of Schedule 1 and Schedule 2. The proposed COPD-MS model can coordinate the operation characteristics and maintenance requirement of transmission lines, and explore the potential economic benefits by coordinately formulating the maintenance and power transmission schedules of transmission lines.

TABLE V
COMPARISON OF RESULTS BY DIFFERENT SCHEDULES

Model	Objective value (10^4 ¥)	Maintenance cost (10^4 ¥)	Transmission loss (MWh)
Proposed COPD-MS	147.91	99.81	717.85
Existing (Schedule 1)	158.26	106.60	734.26
Existing (Schedule 2)	153.59	103.72	729.43

4) Computational Performance of GBD-RA Algorithm

The solution results obtained by the GBD-RA algorithm, PSO algorithm, GBD algorithm, and the directly-solving algorithm are shown in Table VI.

TABLE VI
COMPARISON OF SOLUTION RESULTS BY DIFFERENT ALGORITHMS

Algorithm	Objective value (10^4 ¥)	Number of iterations	CPU time (s)	
			Sub-problem	Master problem
Directly-solving	148.28		13582	
PSO	148.62		5273	
GBD	148.34	13	6852 (1574)	813
GBD-RA	147.91	14	6103 (836)	79

Note: the values in "()" represent the CPU time using parallel computing technology.

The SBB commercial solver is used to solve the optimization model (19) in the directly-solving algorithm. In the PSO algorithm, the swarm size is set to be 80, the inertia weight is set to be 20, the learning factors are set to be 1.5, and the maximum iteration is set to be 200. The maintenance schedules of transmission lines by different algorithms are shown in Table VII. It can be observed that the objective function

values obtained by the GBD-RA algorithm are better than others, indicating that it can obtain an optimal solution with high quality of the original problem. Moreover, the GBD-RA algorithm and GBD algorithm have much lower CPU time consumption than the other two. By using parallel computing technology to solve the sub-problem of each time period independently, the solution time of the sub-problems can be further reduced.

TABLE VII
COMPARISON OF MAINTENANCE SCHEDULES OF TRANSMISSION LINES BY DIFFERENT ALGORITHMS

Algorithm	Starting time of maintenance (hour)						
	AC (31-1)	AC (14-15)	AC (22-21)	LCC (4-3)	VSC(19)	VSC(24)	VSC(16)
Directly-solving	121	168	435	29, 253	393, 581	393, 581	393, 581
PSO	126	157	431	27, 255	402, 591	402, 591	402, 591
GBD	124	159	429	33, 248	390, 585	390, 585	390, 585
GBD-RA	118	164	433	30, 252	396, 587	396, 587	396, 587

Note: DC transmission lines have two starting time of maintenance for their two poles.

The changes of objective values by using the GBD-RA algorithm and the GBD algorithm during the iteration process are shown in Fig. 10. It can be observed that the number of iterations and the changes of objective values of these two algorithms are close. By using the RA algorithm in solving the master problem, the master problem is successfully solved in 12 out of 14 iterations, and the CPU time consumption for solving the master problem is reduced from 813 s to 79 s. This is because the RA algorithm utilizes the solution of the master problem from the last iteration and the added Benders cut constraint to obtain the solution of current iteration efficiently, without having to directly solve the master problem (34) by the optimization solver GUROBI.

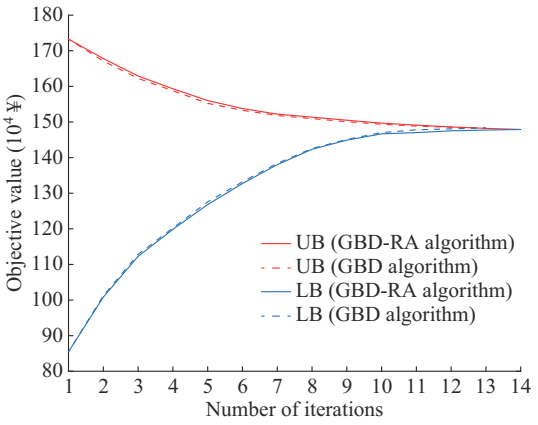

Fig. 10. Changes of objective values by using GBD-RA algorithm and GBD algorithm during iteration process.

5) Solution Result of Proposed COPD-MS Model Considering Uncertainties of Renewable Energy

When considering the uncertainties of renewable energy, the scenario-based method is used in the proposed COPD-MS model to deal with the power output fluctuations of renewable energy stations [31]. Assume that the generators on bus 32 and bus 35 are substituted by a photovoltaic station and a wind farm, respectively. The power output fluctuations of renewable energy stations follow normal distributions, and the standard deviations are set as 20% of the predicted values. Latin hypercube sampling method is used to generate a series of scenarios. In addition, it is necessary to add the scenario transition constraints of the maximum adjustable power by each transmission line between the predicted scenario and each sampling scenario. Under different number of sampling scenarios, the solution results considering the uncertainties of renewable energy are compared in Table VIII. It can be observed that compared with the results in Table V, the objective value and transmission loss of the proposed COPD-MS model with the scenario-based method become greater, which leads to the increasing cost for dealing with the uncertainties of renewable energy. However, the secure operation constraints of paralleled AC/DC transmission channels in the renewable energy fluctuation scenarios can be satisfied.

TABLE VIII
SOLUTION RESULTS CONSIDERING UNCERTAINTIES OF RENEWABLE ENERGY

Number of sampling scenarios	Objective value (10^4 ¥)	Maintenance cost (10^4 ¥)	Transmission loss (MWh)
10	149.62	99.81	734.28
20	150.85	99.81	746.35
30	151.44	99.81	755.71

B. Actual 1524-bus Large-scale AC/DC Hybrid Power System

To demonstrate the scalability of the proposed COPD-MS model, it is tested on an actual 1524-bus large-scale AC/DC hybrid power system. As shown in Fig. 11, the system includes 1524 buses and 227 generators. The system consists of 10 LCC-HVDC transmission lines, 1 three-terminal VSC-MTDC transmission line, and 8 AC transmission lines. Taking the total power exchange schedules of Yunnan, Guizhou, and Guangdong transmission sections in April 2022 (30 days, 720 time periods) as an example, the total power exchange schedule curves are shown in Fig. 12. Considering that it is impossible to complete the maintenance of all transmission lines within one month due to the large number of transmission lines in the system, some transmission lines for maintenance in this month are selected, as shown in Table IX.

1) Solution Result of Proposed COPD-MS Model

By using the GBD-RA algorithm, the maintenance and power transmission schedules of each transmission line can be obtained, as shown in Figs. 13-15. Similar to the results of the modified IEEE 39-bus system, it can be observed that the maintenance of the transmission lines is scheduled on or around the weekends, especially for the VSC(Kun-Liu-Long) transmission line with a high rated capacity. Both LCC-HVDC and VSC-MTDC transmission lines adopt the monopolar maintenance modes to reduce the influence on completing the power transmission schedules.

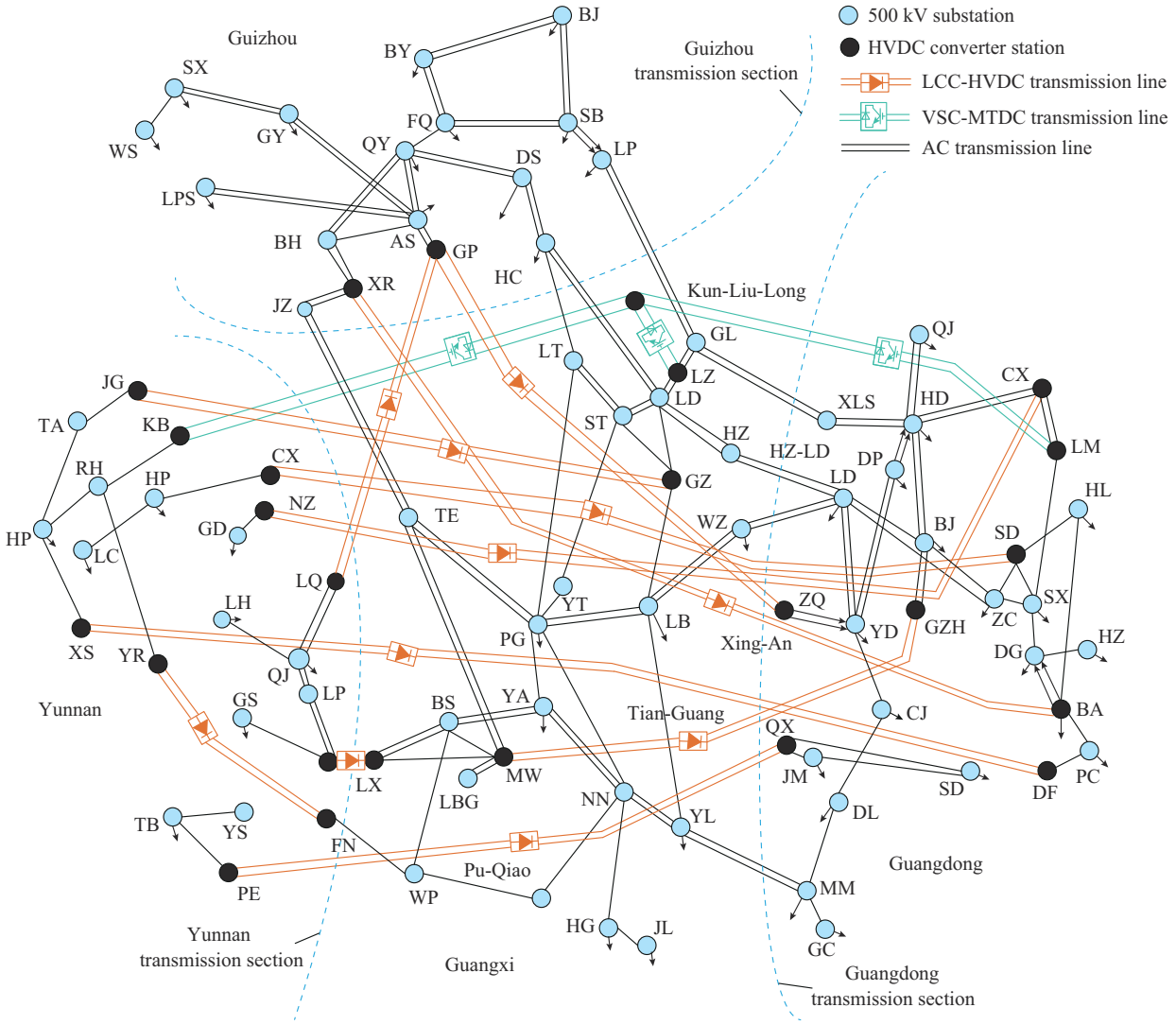

Fig. 11. Structure diagram of actual 1524-bus large-scale AC/DC hybrid power system.

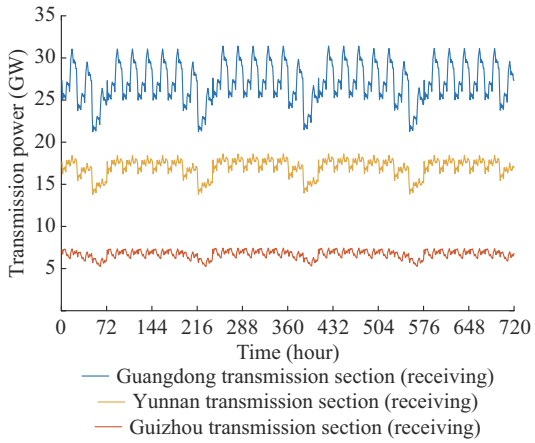

Fig. 12. Monthly power exchange schedule curves of regional sections in actual 1524-bus large-scale AC/DC hybrid power system.

From Fig. 13, it can be observed that for AC transmission lines, AC(GL-XLS) with a short distance and small resistance has a higher transmission power schedule, while the AC(HZ-LD) with a long distance and large resistance has a lower transmission power schedule.

TABLE IX
DATA OF TRANSMISSION LINES FOR MAINTENANCE IN ACTUAL 1524-BUS LARGE-SCALE AC/DC HYBRID POWER SYSTEM

Transmission line	$T_{sm,\min}$ (hour)	$T_{sm,\max}$ (hour)	T_{mR} (hour)	$c_{m,t}$ (10^5 ¥)		Rated power (MW)
				Weekday	Weekend	
AC(GL-XLS)[1]	169	409	72	1.4	1.9	1500
AC(GL-XLS)[2]	97	361	72	1.4	1.9	1500
AC(HZ-LD)[1]	1	120	72	1.2	1.6	1000
AC(HZ-LD)[2]	577	672	72	1.2	1.6	1000
LCC(Tian-Guang)	49	576	72×2	1.8	2.4	1800
LCC(Pu-Qiao)	121	600	72×2	2.5	3.0	5000
LCC(Xing-An)	241	648	72×2	2.2	2.7	3000
VSC(KB)	145	624	96×2	3.0	3.5	8000
VSC(LZ)	145	624	96×2	3.0	3.5	3000
VSC(LM)	145	624	96×2	3.0	3.5	5000

Note: the superscripts "1" and "2" represent AC transmission lines AC(GL-XLS) and AC(HZ-LD) are double-circuit lines; and VSC(KB), VSC(LZ), and VSC(LM) are three converter stations of the VSC(Kun-Liu-Long) transmission line.

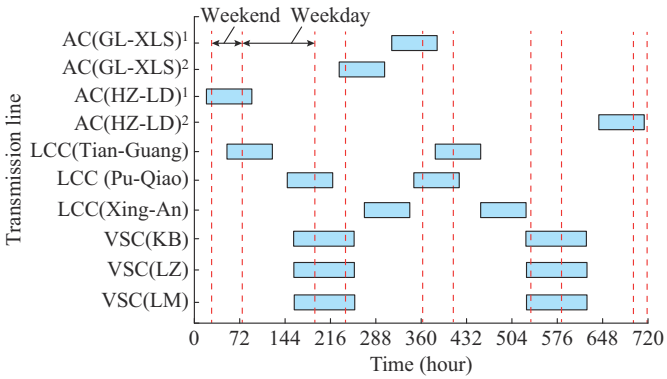

Fig. 13. Maintenance schedules of different transmission lines in actual 1524-bus large-scale AC/DC hybrid power system.

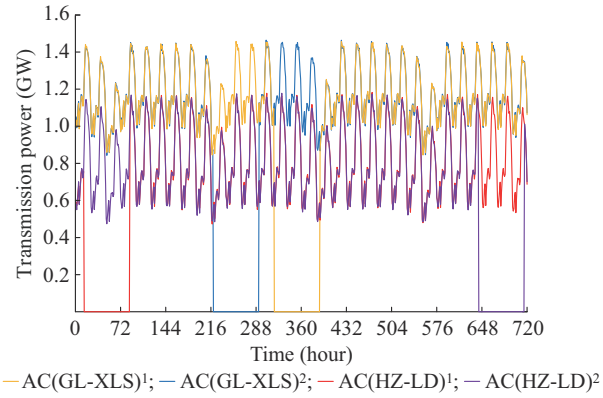

Fig. 14. Power transmission schedules of AC transmission lines in actual 1524-bus large-scale AC/DC hybrid power system.

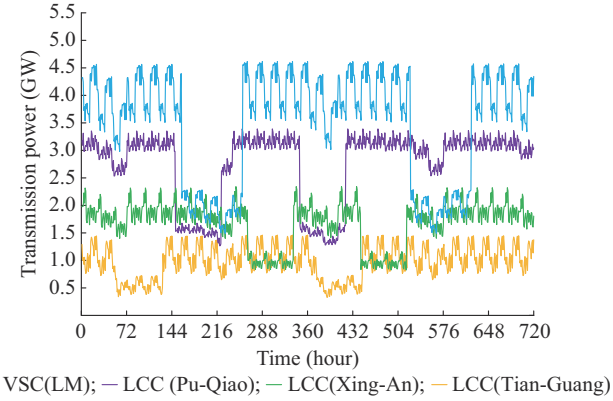

Fig. 15. Power transmission schedules of DC transmission lines in actual 1524-bus large-scale AC/DC hybrid power system.

For DC transmission lines, the transmission power of ±800 kV DC transmission lines such as LCC(Pu-Qiao) and VSC(Kun-Liu-Long) is higher, while the transmission power of ±500 kV DC transmission lines with higher resistance such as LCC(Tian-Guang) and LCC(Xing-An) is lower, which can reduce the total active power loss of all the paralleled AC/DC transmission channels and improve the economic benefits of the system.

2) Computational Performance of GBD-RA Algorithm

For the actual 1524-bus large-scale AC/DC hybrid power system, it cannot be solved directly by using the existing optimization solvers due to the large-scale data. Table X shows the solution results obtained by using the GBD algorithm and the GBD-RA algorithm by using parallel computing technology, the solution time of the sub-problems of multiple time intervals is significantly reduced. Moreover, the computational efficiency can be furthered improved by using more threads.

TABLE X
COMPARISON OF SOLUTION RESULTS BY DIFFERENT ALGORITHMS IN ACTUAL 1524-BUS LARGE-SCALE AC/DC HYBRID POWER SYSTEM

Algorithm	Objective value (10^8 ¥)	Iteration number	CPU time	
			Sub-problem (hour)	Master problem (s)
GBD	8.54	18	25.35 (4.09)	2538
GBD-RA	8.46	17	24.74 (3.48)	136

Note: the values in the "()" represent the CPU time using parallel computing technology.

It can be observed that the GBD-RA algorithm can still be applied to efficiently obtain the solution of the proposed COPD-MS model for large-scale AC/DC power systems. Moreover, as the problem scale increases, the advantage of the RA algorithm in improving the computational efficiency of the master problem is more obvious. This is because in large-scale AC/DC power systems, the master problem includes more variables and constraints, and the GBD algorithm takes more time to solve the master problem during the iteration, while by using the RA algorithm, the solution of the master problem can be efficiently obtained during the iteration.

The changes of objective values by using the GBD-RA algorithm and GBD algorithm during the iteration process in the actual 1524-bus large-scale AC/DC hybrid power system are shown in Fig. 16. It can be observed that the changes of objective values of the two algorithms are close. By using the RA algorithm to solve the master problem, there are 16 times the master problem being successfully solved in the total 17 iterations, and the CPU time for solving the master problem is reduced from 2538 s to 136 s.

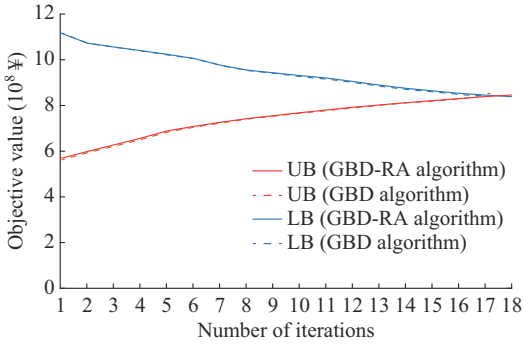

Fig. 16. Changes of objective value by using GBD-RA algorithm and GBD algorithm during iteration process in actual 1524-bus large-scale AC/DC hybrid power system.

V. CONCLUSION

A COPD-MS model of multiple paralleled transmission

channels in an AC/DC power system is established, and the GBD-RA algorithm is proposed to solve the optimization model efficiently and reliably. The proposed COPD-MS model formulates maintenance and power transmission schedules simultaneously, which can improve the economic benefits of the system operation and reduce the influence of line maintenance on completing the given power exchange schedules. Compared with the existing model, the objective value of the proposed COPD-MS model has been improved by 6.5% and 6.3% in cases 1 and 2, respectively. In the GBD-RA algorithm, the convex relaxation of non-convex constraints in the sub-problems can effectively ensure the reliable convergence. In addition, by directly obtaining the solution of the master problem in each iteration, the computational time is significantly reduced by 90.3% and 94.6% in cases 1 and 2, respectively.

With the increasing penetration of renewable energy sources, the power output fluctuations of renewable energy sources will result in the uncertain fluctuations in the transmission power of the AC transmission lines, affecting the secure operation of the system. How to establish a COPD-MS model considering the uncertainty of renewable energy and solve this uncertain optimization model is a possible direction of the future work.

REFERENCES

[1] M. Wang, T. An, H. Ergun *et al*., "Review and outlook of HVDC grids as backbone of transmission system," *CSEE Journal of Power and Energy Systems*, vol. 7, no. 4, pp. 797-810, Jul. 2021.

[2] R. Chen, D. Ke, Y. Sun *et al*., "Hierarchical frequency-dependent chance constrained unit commitment for bulk AC/DC hybrid power systems with wind power generation," *Journal of Modern Power Systems and Clean Energy*, vol. 11, no. 4, pp. 1053-1064, Jul. 2023.

[3] W. Xiang, M. Yang, and J. Wen, "DR-MMC hub based hybrid AC/DC collection and HVDC transmission system for large-scale offshore wind farms," *Journal of Modern Power Systems and Clean Energy*, doi: 10.35833/MPCE.2024.000229

[4] N. Moslemi, M. Kazemi, S. M. Abedi *et al*., "Maintenance scheduling of transmission systems considering coordinated outages," *IEEE Systems Journal*, vol. 12, no. 4, pp. 3052-3062, Dec. 2018.

[5] Y. Fu, M. Shahidehpour, and Z. Li, "Security-constrained optimal coordination of generation and transmission maintenance outage scheduling," *IEEE Transactions on Power Systems*, vol. 22, no. 3, pp. 1302-1313, Aug. 2007.

[6] H. Ergun, J. Dave, D. van Hertem *et al*., "Optimal power flow for AC-DC grids: formulation, convex relaxation, linear approximation, and implementation," *IEEE Transactions on Power Systems*, vol. 34, no. 4, pp. 2980-2990, Jul. 2019.

[7] Z. Yang, H. Zhong, A. Bose *et al*., "Optimal power flow in AC-DC grids with discrete control devices," *IEEE Transactions on Power Systems*, vol. 33, no. 2, pp. 1461-1472, Mar. 2018.

[8] J. Cao, W. Du, H. Wang *et al*., "Minimization of transmission loss in meshed AC/DC grids with VSC-MTDC networks," *IEEE Transactions on Power Systems*, vol. 28, no. 3, pp. 3047-3055, Aug. 2013.

[9] S. Bahrami, F. Therrien, V. W. S. Wong *et al*., "Semidefinite relaxation of optimal power flow for AC-DC grids," *IEEE Transactions on Power Systems*, vol. 32, no. 1, pp. 289-304, Jan. 2017.

[10] Q. Li, M. Liu, and H. Liu, "Piecewise normalized normal constraint method applied to minimization of voltage deviation and active power loss in an AC-DC hybrid power system," *IEEE Transactions on Power Systems*, vol. 30, no. 3, pp. 1243-1251, May 2015.

[11] H. Huang, M. Zhou, S. Zhang *et al*., "Exploiting the operational flexibility of wind integrated hybrid AC/DC power systems," *IEEE Transactions on Power Systems*, vol. 36, no. 1, pp. 818-826, Jan. 2021.

[12] Z. Li, W. Wu, M. Shahidehpour *et al*., "Adaptive robust tie-line scheduling considering wind power uncertainty for interconnected power systems," *IEEE Transactions on Power Systems*, vol. 31, no. 4, pp. 2701-2713, Jul. 2016.

[13] S. Lin, Z. Yang, G. Fan *et al*., "A mixed-integer second-order cone programming algorithm for the optimal power distribution of AC-DC parallel transmission channels," *Energies*, vol. 12, no. 19, p. 3605, Sept. 2019.

[14] J. Mei, G. Zhang, D. Qi *et al*., "Accelerated solution of the transmission maintenance schedule problem: a Bayesian optimization approach," *Global Energy Interconnection*, vol. 4, no. 5, pp. 493-500, Oct. 2021.

[15] D. Xu, Z. Cai, Q. Cheng *et al*., "Security-constrained transmission maintenance optimization considering generation and operational risk costs," *Journal of Modern Power Systems and Clean Energy*, vol. 12, no. 3, pp. 767-781, May 2024.

[16] L. S. S. Martin, J. Yang, and Y. Liu, "Hybrid NSGA III/dual simplex approach to generation and transmission maintenance scheduling," *International Journal of Electrical Power & Energy Systems*, vol. 135, p. 107498, Feb. 2022.

[17] F. Moinian and M. T. Ameli, "A reliability-based approach for integrated generation and transmission maintenance coordination in restructured power systems," *Electric Power Systems Research*, vol. 206, p. 107737, May 2022.

[18] W. Zhang, B. Hu, K. Xie *et al*., "Short-term transmission maintenance scheduling considering network topology optimization," *Journal of Modern Power Systems and Clean Energy*, vol. 10, no. 4, pp. 883-893, Jul. 2022.

[19] Y. Wang, Z. Li, M. Shahidehpour *et al*., "Stochastic co-optimization of midterm and short-term maintenance outage scheduling considering covariates in power systems," *IEEE Transactions on Power Systems*, vol. 31, no. 6, pp. 4795-4805, Nov. 2016.

[20] M. K. C. Marwali and S. M. Shahidehpour, "Integrated generation and transmission maintenance scheduling with network constraints," *IEEE Transactions on Power Systems*, vol. 13, no. 3, pp. 1063-1068, Aug. 1998.

[21] M. Y. El-Sharkh and A. A. El-Keib, "Maintenance scheduling of generation and transmission systems using fuzzy evolutionary programming," *IEEE Transactions on Power Systems*, vol. 18, no. 2, pp. 862-866, May 2003.

[22] Y. Wang, H. Zhong, Q. Xia *et al*., "An approach for integrated generation and transmission maintenance scheduling considering $N-1$ contingencies," *IEEE Transactions on Power Systems*, vol. 31, no. 3, pp. 2225-2233, May 2016.

[23] J. Li, L. Zheng, and X. Tang, "Network maintenance scheduling with maintenance resource constraints," in *Proceedings of 2022 IEEE International Conference on Unmanned Systems* (*ICUS*), Guangzhou, China, Oct. 2022, pp. 1420-1425.

[24] Y. Huang, Q. Xin, X. Zhao *et al*., "Research on fast conversion method of metallic return to earth return operation mode in HVDC system," in *Proceedings of 2018 International Conference on Power System Technology* (*POWERCON*), Guangzhou, China, Nov. 2018, pp. 2591-2595.

[25] H. Fudeh and C. M. Ong, "A simple and efficient AC-DC load-flow method for multiterminal DC systems," *IEEE Transactions on Power Apparatus and Systems*, vol. PAS-100, no. 11, pp. 4389-4396, Nov. 1981.

[26] R. Martínez-Parrales, C. R. Fuerte-Esquivel, B. A. Alcaide-Moreno *et al*., "A VSC-based model for power flow assessment of multi-terminal VSC-HVDC transmission systems," *Journal of Modern Power Systems and Clean Energy*, vol. 9, no. 6, pp. 1363-1374, Nov. 2021.

[27] A. M. Geoffrion, "Generalized Benders decomposition," *Journal of Optimization Theory and Applications*, vol. 10, no. 4, pp. 237-260, 1972.

[28] A. J. Conejo, E. Castillo, and R. Mínguez, *Decomposition Techniques in Mathematical Programming*. Berlin: Springer, 2006.

[29] S. Lin, Y. Yang, M. Liu *et al*., "Static voltage stability margin calculation of power systems with high wind power penetration based on the interval optimisation method," *IET Renewable Power Generation*, vol. 14, no. 10, pp. 1728-1737, Jul. 2020.

[30] W. Liang, S. Lin, J. Liu *et al*., "Multi-objective mixed-integer convex programming method for the siting and sizing of UPFCs in a large-scale AC/DC transmission system," *IEEE Transactions on Power Systems*, vol. 38, no. 6, pp. 5671-5686, Nov. 2023.

[31] J. Liu, S. Lin, S. He *et al*., "Multiobjective optimal dispatch of mobile energy storage vehicles in active distribution networks," *IEEE Systems Journal*, vol. 17, no. 1, pp. 804-815, Mar. 2023.

Jie Liu received the B.S. degrees in electrical engineering from the South China University of Technology, Guangzhou, China, in 2020. He is currently pursuing the M.S. degree with the School of Electric Power Engineering,

South China University of Technology. His research interests include power system optimization, operation, and control.

Shunjiang Lin received the B.S. degree in electrical engineering from the South China University of Technology, Guangzhou, China, in 2003, and the Ph. D. degree in electrical engineering from Hunan University, Changsha, China, in 2008. He is currently an Associate Professor with the School of Electric Power Engineering, South China University of Technology. His research interests include power system optimization, operation, and control.

Weikun Liang received the B.S. degrees in electrical engineering from the South China University of Technology, Guangzhou, China, in 2020. He is currently pursuing the Ph.D. degree with the School of Electric Power Engineering, South China University of Technology. His research interests include power system optimization, operation, and control.

Yanghua Liu received the Ph.D. degree in electrical engineering from Hunan University, Changsha, China, in 2010. She is currently a Lecturer with the School of Electromechanical Engineering, Guangdong Polytechnic Normal University, Guangzhou, China. Her research interests include optimal operation and control of power systems and electricity market.

Mingbo Liu received the B.S. degree from the Huazhong University of Science and Technology, Wuhan, China, in 1985, the M.S. degree from the Harbin Institute of Technology, Harbin, China, in 1988, and the Ph.D. degree from Tsinghua University, Beijing, China, in 1992. He is currently a Professor with the South China University of Technology, Guangzhou, China. His research interests include energy management and operation control of power systems.